Stem Cell Reports
Resource
ISSCR
OPEN ACCESS

Modeling sex differences in humans using isogenic induced pluripotent stem cells

Ithai Waldhorn,[1] Tikva Turetsky,[1] Debora Steiner,[1] Yaniv Gil,[1] Hadar Benyamini,[2] Michal Gropp,[1] and Benjamin E. Reubinoff[1,3,*]
[1]Hadassah Stem Cell Research Center, Goldyne Savad Institute of Gene Therapy, Hadassah Hebrew University Medical Center, Jerusalem, Israel
[2]Bioinformatics Unit of the I-CORE at Hebrew University and Hadassah Medical Center, Jerusalem, Israel
[3]Department of Obstetrics and Gynecology, Ein Kerem, Hadassah Hebrew University Medical Center, Jerusalem, Israel
*Correspondence: benr@hadassah.org.il
https://doi.org/10.1016/j.stemcr.2022.10.017

SUMMARY

Biological sex is a fundamental trait influencing development, reproduction, pathogenesis, and medical treatment outcomes. Modeling sex differences is challenging because of the masking effect of genetic variability and the hurdle of differentiating chromosomal versus hormonal effects. In this work we developed a cellular model to study sex differences in humans. Somatic cells from a mosaic Klinefelter syndrome patient were reprogrammed to generate isogenic induced pluripotent stem cell (iPSC) lines with different sex chromosome complements: 47,XXY/46,XX/46,XY/45,X0. Transcriptional analysis of the hiPSCs revealed novel and known genes and pathways that are sexually dimorphic in the pluripotent state and during early neural development. Female hiPSCs more closely resembled the naive pluripotent state than their male counterparts. Moreover, the system enabled differentiation between the contributions of X versus Y chromosome to these differences. Taken together, isogenic hiPSCs present a novel platform for studying sex differences in humans and bear potential to promote gender-specific medicine in the future.

INTRODUCTION

In recent years, the awareness of gender medicine is rising. It is now well established that disease incidence, clinical presentation, and outcome are sex dependent (Hao et al., 2019; Lichtman et al., 2018; Whitacre, 2001). In addition, adverse drug reactions are sex dependent (Yu et al., 2016), and several drugs were withdrawn from the market by the US Food and Drug Administration (FDA) because of their gender-specific hazardous effects, usually on women (Pollitzer, 2013). Genome-wide association studies (GWAS) (Khramtsova et al., 2019) have revealed complex human traits such as metabolism (Charchar et al., 2012; Ge et al., 2017; Heid et al., 2010; Winkler et al., 2015), immunity (Case et al., 2013; Kamitaki et al., 2020; Krementsov et al., 2017; Kukurba et al., 2016), and anthropometrics (Traglia et al., 2017) to be sex dependent. Although some of the sex differences arise from hormonal effects (Gurvich et al., 2018), it is now acknowledged that many differences are due to sex chromosome complement (Arnold, 2012). Studying the effects of sex chromosome complement on gene expression and biological phenotypes is impeded by variation in genetic background. Therefore a large sample size is needed to identify sex-related differences (Ronen and Benvenisty, 2014). To date, there is no human model to study sex differences that can overcome the variation in genetic background.

In this work we sought to develop a novel cellular model that is based on a unique sex chromosome complement of a subgroup of Klinefelter syndrome patients. Klinefelter syndrome is characterized by an additional X chromosome in males (47,XXY). Approximately 15% of these patients have a mosaic karyotype of 47,XXY/46,XY because of trisomic rescue in early development (Frühmesser and Kotzot, 2011). In rare cases, patients harbor a karyotype of 47,XXY/46,XY/46,XX (Al-Awadi et al., 1986; Bergman et al., 1969; Ekwall et al., 1971; Hersmus et al., 2012; Mark et al., 1999; Zamora et al., 2002). In this study, 47,XXY/46,XY/46,XX EBV-immortalized B cells from a single Klinefelter syndrome patient were exploited to generate isogenic human induced pluripotent stem cells (hiPSCs) with different sex chromosome complements. This model was used to study sex differences in gene expression of undifferentiated and early neural differentiated hiPSCs, and to distinguish between the effects of X and Y chromosomes on autosomal gene expression.

RESULTS

Generation of isogenic hiPSC lines with different sex chromosome complements

With the goal of generating isogenic hiPSC lines with different sex chromosome complements, an EBV-immortalized B cell line derived from a mosaic Klinefelter syndrome patient was subjected to fluorescence *in situ* hybridization (FISH) analysis, which showed that the cell line was composed of 47,XXY (71.5%), 46,XY (25%), and 46,XX (3.5%) cells (Figure S1A). Single B cells were reprogrammed to iPSCs, as single cells via nucleofection with four plasmids

overexpressing *SOX2*, POU5F1 (*OCT4*), *KLF4*, *LIN28A*, MYCL, SV40LT, and shTP53 (Barrett et al., 2014). Following reprogramming, hiPSC colonies were screened for sex chromosome complement number, determined by the presence of *SRY* and *XIST* genes encoded by the X and Y chromosomes, respectively (Figure S1B). Of 100 colonies, 52 were 47,XXY, 45 were 46,XY, and one was 46,XX. Surprisingly, one 45,X0 colony representing an elimination of the X chromosome and one 93,XXXXY colony that was probably generated by fusion of 46,XX and 47,XXY cells were identified. To generate additional 46,XX cell lines, another 250 colonies were screened for the absence of the Y chromosome; two 46,XX colonies were identified. The screening results for the selected clones were confirmed by G banding, which showed normal karyotype (Figure S1C). Altogether, nine isogenic hiPSC lines were generated: three 46,XX, three 46,XY, two 47,XXY, and one 45,X0 cell lines.

Characterization of isogenic hiPSC lines

When cultured on human foreskin fibroblast feeders, the isogenic hiPSCs (passages 20–25) showed typical morphology and alkaline phosphatase activity (Figures S1D). The majority of the cells expressed the key pluripotency transcription factor OCT4, as well as the pluripotency-associated cell surface markers TRA-1-61 and TRA-1-80 (Figure 1A). All cell lines were pluripotent, as demonstrated by their potential to differentiate *in vitro* and *in vivo* into cells representing the three embryonic germ layers (Figures 1B and 1C). XX and XXY isogenic hiPSCs were X inactivated, as demonstrated by perinuclear single-focus staining of H3K27me3 (Figure 1D). PCR for viral DNA showed absence of EBV-related genes, indicating that the viral elements were eliminated during reprogramming (Figure S1E). Short tandem repeat (STR) fingerprinting and human leukocyte antigen (HLA) typing of the hiPSCs demonstrated autosomally identical samples, confirming that the hiPSC lines were isogenic (profiles are not shown to maintain donor confidentiality). In addition, SNP analysis showed matched identity between all samples (Table S1A). Taken together, the protocol used yielded isogenic hiPSCs with different sex chromosome complements. The hiPSCs were EBV free, pluripotent, undifferentiated, and X inactivated when cultured on human feeders.

Gene expression analysis of XX and XY isogenic hiPSCs

Because of the early onset of sex differences during development (Petropoulos et al., 2016), gene expression in the undifferentiated isogenic hiPSCs was compared. To this end, RNA from the isogenic hiPSC lines cultured on human feeders was extracted after verifying using fluorescence-activated cell sorting (FACS) that >93% of the cells were TRA-1-81^{+} (Figure S2A), and RNA sequencing (RNA-seq) was performed. The RNA-seq analysis detected 63,899 transcripts (95.3% autosomal, 3.7% X linked, and 1% Y linked). Principal-component analysis (PCA) of XX and XY hiPSCs showed that the hiPSC lines clustered by sex chromosome complement for autosomal and sex-linked genes (Figure S2B). Differential gene expression analysis (adjusted p value < 0.10) detected 313 genes differentially expressed in XY versus XX samples, with 247 DEGs (79%) significantly upregulated in XX compared with XY (Figures 2A and 2B; Table S1B). Most of the differentially expressed genes (DEGs) were autosomal genes (n = 286), while only 10 were X-linked genes and 15 were Y-linked genes, of which 10 had X-linked paralogs. As expected, *XIST*, a major effector of X inactivation, showed the highest XX/XY expression ratio, while Y-linked genes such as *SRY* were expressed in cell lines containing the Y chromosome. *MMP3*, an autosomal gene that was shown to be the most differentially expressed autosomal gene between the sexes in multiple tissues (Melé et al., 2015), was also differentially expressed in the isogenic hiPSCs (Table S1B). The differential expression of a subset of autosomal and sex-linked DEGs, selected according to their adjusted p value and fold change was validated using qRT-PCR (Figure S2C).

Comparison of the RNA-seq data with published autosomal DEGs identified using microarray data of multiple conventional XX and XY human embryonic stem cell (hESC) lines (Ronen and Benvenisty, 2014) (see supplemental experimental procedures) found 73% agreement in expression directionality between the published autosomal DEGs and our gene expression data (p = 2.1e-10; Figure 1C). Next, we tested our own set of autosomal DEGs using transcriptome data of the conventional hESC lines. We found that 72% of the autosomal DEGs had the same expression directionality as in our analysis (p = 3.2e-20; Figure 1D; Table S1C).

A gene set enrichment analysis (GSEA) (Subramanian et al., 2005) was carried out through the Broad Institute GenePattern interface to identify sexually dimorphic gene networks. GSEA identified an enrichment for early estrogen response, adipogenesis, and glycolysis in XX hiPSC, in line with published data (Chen et al., 2012; Kimura et al., 2005; Ronen and Benvenisty, 2014) (Figure 2E). Autosomal genes related to spermatogenesis were enriched in XY hiPSCs, as were cell cycle control gene sets, in line with the higher growth rate observed in early-developing XY embryos compared with XX embryos (Bernardi and Delouis, 1996; Pergament et al., 1994; Valdivia et al., 1993). Other gene sets that were sex biased included inflammatory response, interferon gamma response, and TNF-α signaling (Figure S3A). Further analysis of sex differences using Ingenuity Pathway Analysis (IPA) of DEGs, found a sex bias for pathways related to diseases that are more prevalent in women, such as osteoarthritis and rheumatoid arthritis

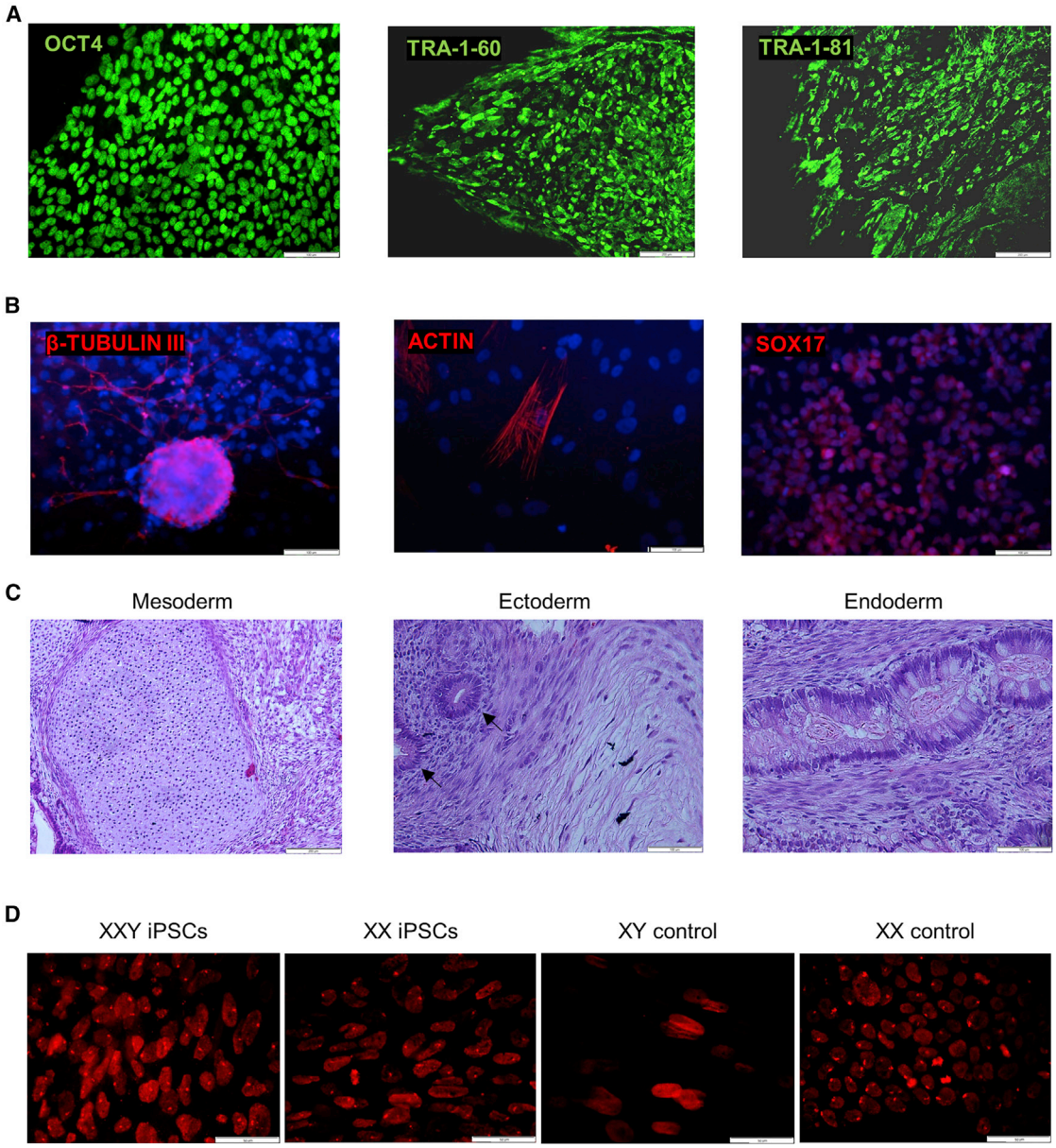

Figure 1. Characterization of isogenic human induced pluripotent stem cell (hiPSC) lines

(A) Immunofluorescence staining for the pluripotency markers OCT4 (scale bar, 100 μm), TRA-1-60, and TRA-1-81 in XY hiPSCs (scale bar, 200 μm).

(B) Immunofluorescence staining following *in vitro* differentiation of XY hiPSCs, showing cells expressing β-tubulin III (neuronal marker, ectoderm), muscle actin (mesoderm), and SOX17 (endoderm). Scale bar, 100 μm.

(C) H&E staining images of teratoma tumors developed following *in vivo* differentiation of XY hiPSCs, showing mesoderm (cartilage; scale bar, 200 μm), ectoderm (neural rosettes; black arrows), and endoderm (columnar glandular epithelium) differentiation (scale bar, 100 μm).

(D) Immunofluorescence staining for H3K27me3, a repressive histone marker of the inactive X chromosome, in XX and XXY hiPSCs. XY fibroblasts and primed XX hPSCs served as controls (scale bar, 50 μm).

(Table S1D). Interestingly, the pathways that were most enriched with sex-biased genes were also reported as the most enriched in an analysis of sex differences in human myocardial tissues (Figure 2F) (Inanloorahatloo et al., 2017). Analysis by chromosomal location found only Y chromosome to be enriched with DEGs (fold enrichment = 3.91, adjusted

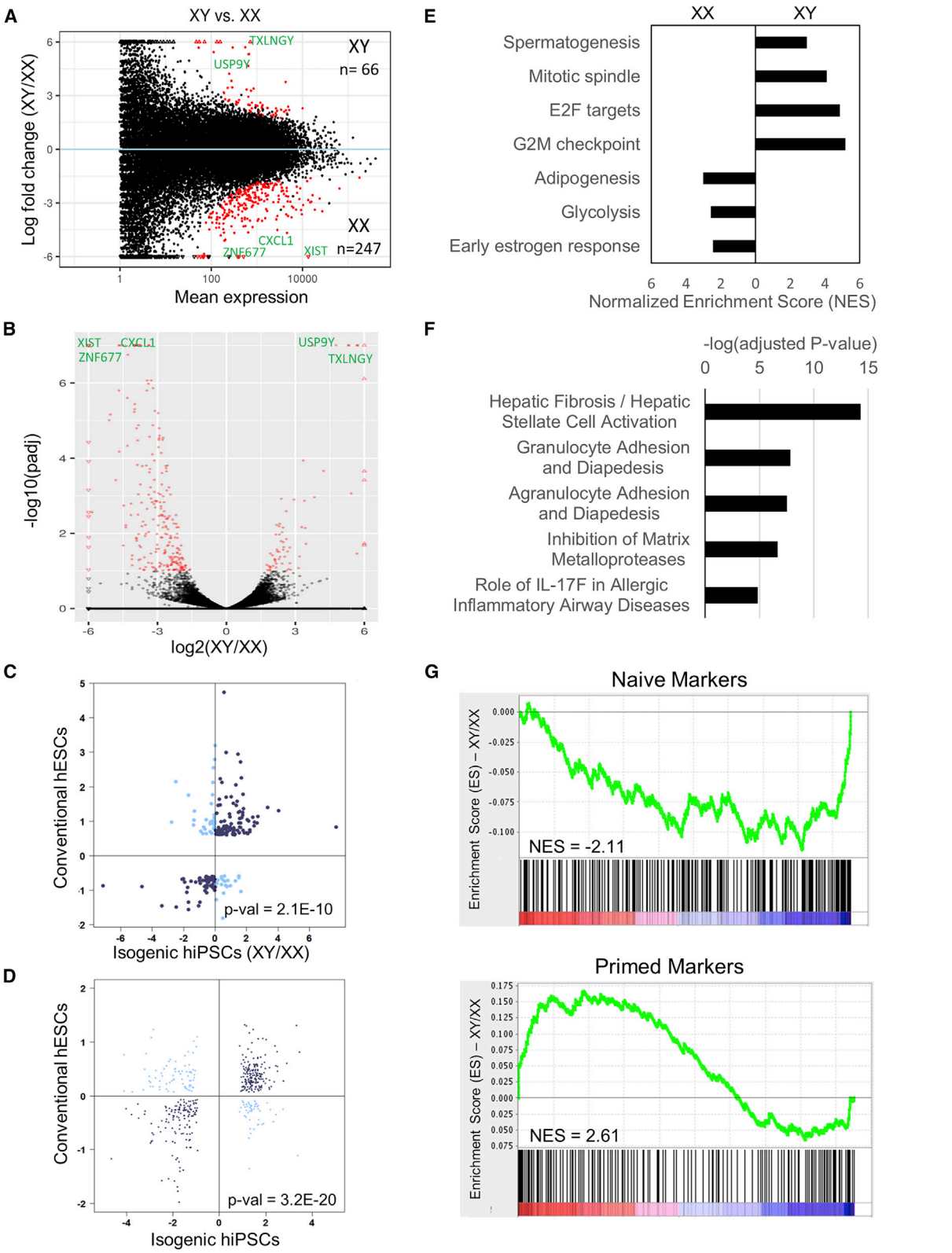

(legend on next page)

p = 0.003). Taken together, the gene expression profiling of the isogenic hiPSC lines recapitulated known sex differences and suggested novel differences between the sexes.

Pluripotency state analysis of the isogenic hiPSCs

Two main states/phases of pluripotency have been defined: "naive" cells that more closely resemble the pre-implantation epiblast and conventional "primed" cells that represent the post-implantation developmental stage. These cells are classified on the basis of differences in gene expression signatures, chromatin states, differentiation capacity, and other properties.

GSEA of the pluripotency state in isogenic male and female hiPSCs cultured on human feeders was tested by gene sets that represent naive and primed states in XX and XY human pluripotent stem cells (hPSCs). The gene sets were generated by selecting the top 500 genes differentially expressed between naive and primed human pluripotent stem cells, on the basis of Stirparo et al. (2018): 316 naive state markers and 184 primed state markers (Table S1E). GSEA revealed that naive state markers were enriched in XX hiPSCs (normalized enrichment score [NES] = −2.1), while primed state markers were enriched in XY hiPSCs (NES = 2.6; Figure 2G). An additional naive gene set, compiled on the basis of published naive markers (Collier et al., 2017; Gafni et al., 2013; Giulitti et al., 2019; Guo et al., 2016; Kilens et al., 2018; Messmer et al., 2019; Nakamura et al., 2016; Pastor et al., 2018; Sperber et al., 2015; Theunissen et al., 2014; Zimmerlin et al., 2016), demonstrated enrichment in XX hiPSCs as well (NES = −3.3; Figure S3B). To validate these findings, the naive gene set was tested using a published transcriptome dataset from conventional hESCs (Ronen and Benvenisty, 2014) and was found to be enriched in XX hESCs compared with XY hESCs (NES = −2.2; Figure S3B). In addition, signaling pathways that are important for induction and maintenance of naive pluripotency in human (Duggal et al., 2015; Yang et al., 2010; Xu et al., 2016) such as JAK-STAT, PI3K/AKT, and WNT signaling pathways were enriched in female compared with male hiPSCs, while the MAPK signaling pathway was enriched in XX hiPSCs (Figure S3C). Taken together, gene expression in female isogenic hiPSCs is slightly closer to naive pluripotency than male hiPSCs.

The effect of sex chromosomes on autosomal genes

The differences between XX and XY can arise from the presence of the Y chromosome, the dose of the X chromosome, or both. To facilitate analysis of the determining factors, two 47,XXY and one 45,X0 hiPSC lines were included in subsequent analyses. The nine cell lines were classified according to X dose (X0 and XY compared with XX and XXY) and chromosome Y presence (X0 and XX compared with XY and XXY; Figure 3A), and their gene expression was analyzed to detect X and Y chromosome effects (see supplemental experimental procedures). As expected, XIST was related to the X dose, while genes located on Y chromosome were attributed to the presence of Y. Of the 313 identified DEGs, 92 genes were related to the presence of Y, while 46 genes were related to the dose of X (Figure 3B; Table S2). Significant effects of both X dose and Y presence were demonstrated for 53 DEGs, such as MMP3. Interacting effects of X and Y chromosomes were noted for 122 DEGs,

Figure 2. Gene expression analysis of XX and XY isogenic hiPSCs

(A) MA plot presenting gene expression differences between XY and XX samples. The mean expression (A) is shown on the x axis, and $\log_2$ fold change (M) is plotted on the y axis. Each gene is represented by a dot. Genes with adjusted p values < 0.10 are shown in red. Three cell lines were tested for each sex.

(B) Volcano plot displaying differentially expressed genes (DEGs) between XX and XY hiPSCs. The y axis reflects the mean expression value of $\log_{10}(q)$, and the x axis displays the $\log_2$ fold change value. Red dots represent significant DEGs.

(C) Correlation between published autosomal DEGs between the sexes, as determined in a conventional hESC study (n = 192) (y axis) (Ronen and Benvenisty, 2014), and our gene expression data (x axis), depicted as a scatterplot of all pairwise $\log_2$ fold changes between the sexes. Dark blue dots represent genes that share the same expression directionality in both studies. Fold change levels were also correlated (rho = 0.38, p = 4E-8).

(D) Correlation between autosomal DEGs (p < 0.10) found in our analysis (n = 448) (x axis) and published transcriptome data from conventional hESCs (y axis) (Ronen and Benvenisty, 2014). Dark blue dots represent genes that share the same expression directionality in both studies.

(E) Gene set enrichment analysis (GSEA) for selected gene sets in XX and XY hiPSCs. The x axis represents the normalized enrichment score (significance was defined as FDR < 0.01 and FWER < 0.1).

(F) Top five differentially expressed pathways for female- and male-biased genes, as determined using Ingenuity Pathway Analysis (IPA). Pathways were selected according to their log of adjusted p value.

(G) GSEA results presented in an enrichment plot for naive and primed state markers in XY compared with XX hiPSCs (NES, normalized enrichment score; FDR < 0.01, FWER < 0.1). The green line represents the enrichment score (ES) of the gene set as a running-sum statistic working down the ranked list of genes. The black vertical bars illustrate the position of genes belonging to the gene set in the ranked list of genes included in the analysis. The colored band represents the degree of correlation of the expression in the gene set (red for a high gene expression and blue for a low gene expression).

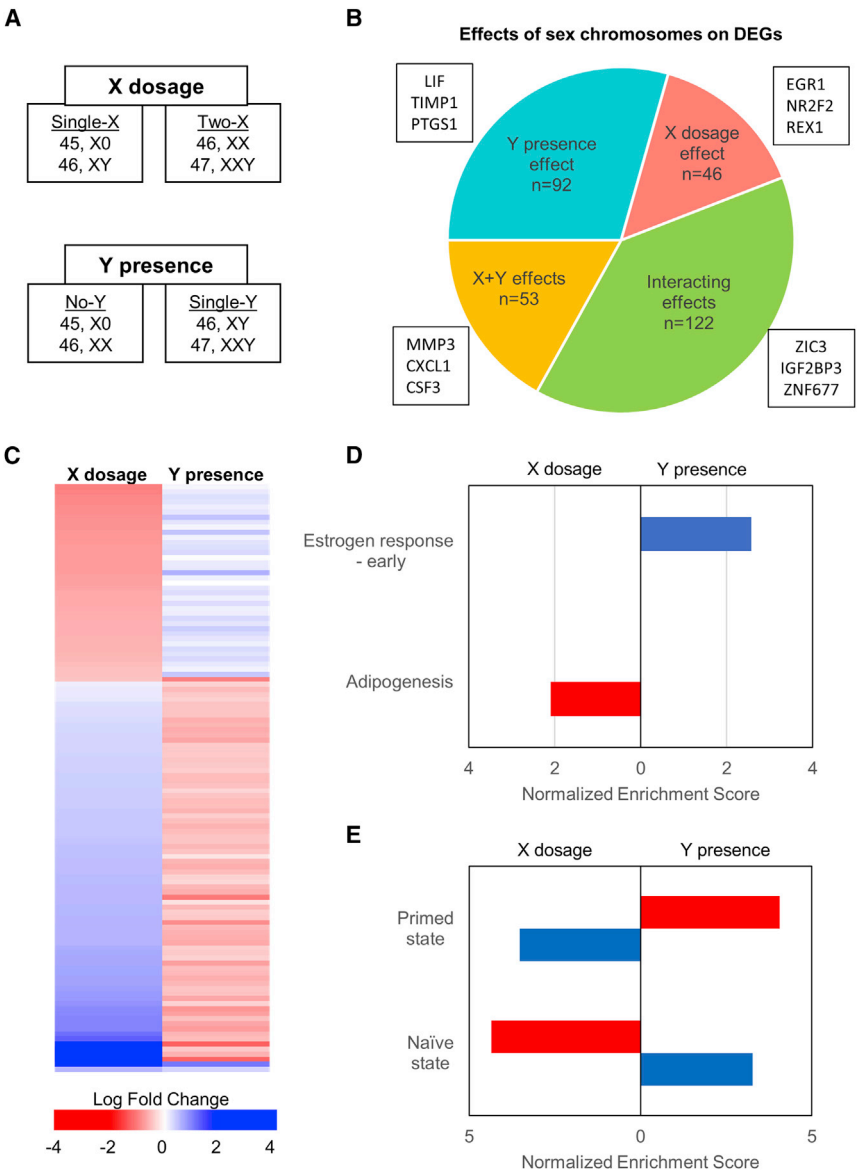

Figure 3. The effect of X and Y chromosomes on autosomal gene expression

(A) hiPSC samples were categorized according to the number of X chromosomes (X dose) and the presence of Y chromosome (Y presence), as determined using RNA-seq of nine isogenic hiPSC lines.

(B) The effect of X dose and Y presence on differentially expressed genes (DEGs). A pie chart representing the number of DEGs that are significantly affected by Y presence (blue), X dose (red), or both (yellow). An additional 122 genes had interacting effects of X and Y chromosomes (green). Representative genes from each group are marked by a black box.

(C) Heatmap of $\log_2$ fold change of 122 DEGs that had interactive inverse effects of X and Y chromosomes. Each row represents a single gene and the opposite effect of X dose (left column) and Y presence (right column) on its expression.

(D) GSEA for significant effects of X dose and Y presence on specific gene sets. Red bars represent an upregulation effect, while blue bars represent downregulation (FDR < 0.01 and FWER < 0.1).

(E) GSEA for X dose and Y presence effects on primed and naive state markers. Red bars represent an upregulation effect, while blue bars represent downregulation (FDR < 0.01 and FWER < 0.1).

which showed inverse correlations to X dose and Y presence, yielding an additive effect that was significant when comparing XX and XY (Figure 3C). For example, FGF8 was upregulated in the presence of two X chromosomes and downregulated by the Y chromosome (both insignificantly); additively, FGF8 was significantly upregulated in XX compared with XY hiPSCs.

Assessment of the effect of X dose and Y presence on gene networks associated an enrichment of an early estrogen response gene set with lack of a Y chromosome and not with X chromosome dose, in line with a previously published work on hESCs (Ronen and Benvenisty, 2014). Adipogenesis gene enrichment was related to X dose, as was shown in mice (Chen et al., 2012) (Figure 3D). The differences in naive and primed gene sets were found to be attributed to both Y presence and X dose (Figure 3E). The effects of X dose and Y presence on other gene sets are shown in Table S2.

Sex differences during neural differentiation

To detect sex differences in human early neural development when sex chromosome complement is the only determinant of sex differences (Turano et al., 2018), the XX and XY hiPSC lines were directed to differentiate towards the neural lineage and subsequently compared. After 14 days of differentiation, the majority of cells acquired neural progenitor phenotype, as demonstrated by the expression of PSA-NCAM (92% ± 3.5%; FACS analysis) and NESTIN (>90%; immunostaining) (Figures 4A and 4B). RNA

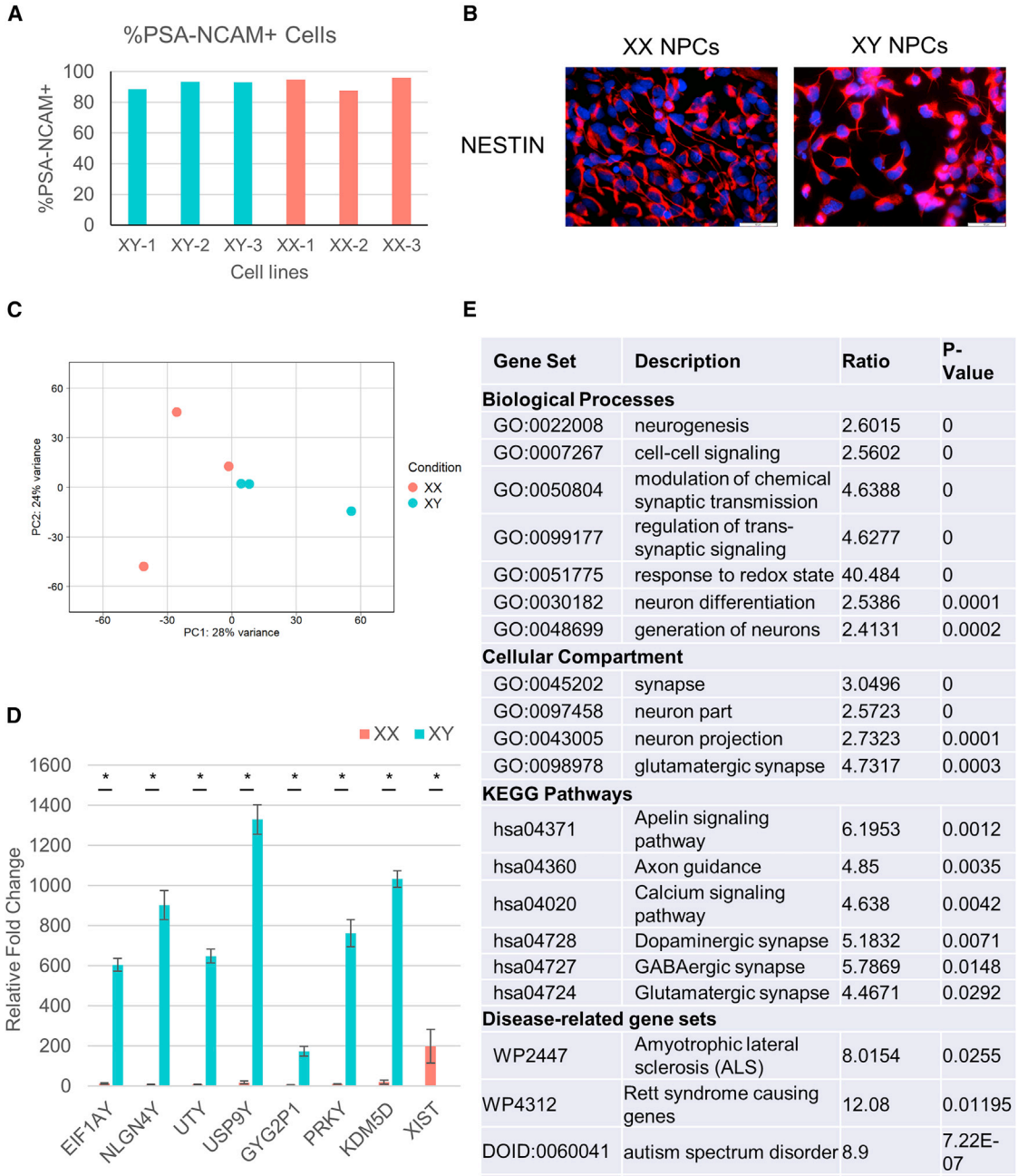

E

Gene Set	Description	Ratio	P-Value
Biological Processes			
GO:0022008	neurogenesis	2.6015	0
GO:0007267	cell-cell signaling	2.5602	0
GO:0050804	modulation of chemical synaptic transmission	4.6388	0
GO:0099177	regulation of trans-synaptic signaling	4.6277	0
GO:0051775	response to redox state	40.484	0
GO:0030182	neuron differentiation	2.5386	0.0001
GO:0048699	generation of neurons	2.4131	0.0002
Cellular Compartment			
GO:0045202	synapse	3.0496	0
GO:0097458	neuron part	2.5723	0
GO:0043005	neuron projection	2.7323	0.0001
GO:0098978	glutamatergic synapse	4.7317	0.0003
KEGG Pathways			
hsa04371	Apelin signaling pathway	6.1953	0.0012
hsa04360	Axon guidance	4.85	0.0035
hsa04020	Calcium signaling pathway	4.638	0.0042
hsa04728	Dopaminergic synapse	5.1832	0.0071
hsa04727	GABAergic synapse	5.7869	0.0148
hsa04724	Glutamatergic synapse	4.4671	0.0292
Disease-related gene sets			
WP2447	Amyotrophic lateral sclerosis (ALS)	8.0154	0.0255
WP4312	Rett syndrome causing genes	12.08	0.01195
DOID:0060041	autism spectrum disorder	8.9	7.22E-07
GSE61476_up	Autism iPSCs-derived Neural Cultures	6.4	1.012E-06

Figure 4. Sex differences during early neural differentiation

(A) FACS analysis for PSA-NCAM expression after 14 days of neural differentiation.

(B) Immunostaining for the neural marker NESTIN (red). Nuclei were counterstained with DAPI (blue) (scale bar, 50 mm).

(C) Principal-component analysis (PCA) plot of XX (red) and XY (blue) isogenic hiPSCs following neural differentiation. Three isogenic hiPSC lines of each sex were analyzed.

(D) RT-PCR analysis of X- and Y-linked genes in XX and XY NPCs. Data represent normalized expression ± SEM of three biological replicates ($p < 0.05$).

(E) Biological function enrichment analysis for genes differentially expressed in female versus male hiPSCs following neural differentiation.

extracted from the neural progenitor cells (NPCs) derived from the isogenic hiPSC lines, showed that the NPCs clustered according to sex chromosome complement (Figure 4C). Differential gene expression analysis (adjusted $p < 0.10$) identified 69 DEGs, of which 71% were upregulated, and 29% were downregulated in XY compared with XX NPCs (Table S3). These results are in line with previous reports showing that during prenatal brain development, most of the DEGs were upregulated in males (O'Brien et al., 2019; Shi et al., 2016). As expected, DEGs included Y-linked genes and *XIST* (Figure 4D). HSD17B7, one of the top 5 autosomal DEGs was upregulated in XY NPCs. This enzyme regulates the biologic potency of estrogen, progesterone, and testosterone. *GRIN3A* and *SF3B1*, another two top-five DEGs and associated with schizophrenia, were upregulated in XY NPSCs. GRIN3A is also associated with cerebral palsy disease. Interestingly, these conditions have a male-biased prevalence (Chounti et al., 2013; Costantine et al., 2012; Greenwood et al., 2016; Ingason et al., 2015; McGrath et al., 2004; Takata et al., 2013).

A functional annotation analysis using WebGestalt and EnrichR (Kuleshov et al., 2016; Liao et al., 2019) of genes differentially expressed in NPCs derived from the male versus female isogenic hiPSCs ranked neurogenesis, cell-cell signaling, synaptic transmission, transsynaptic signaling, response to redox state, and neuronal differentiation as the top most significant differentiating biological processes (Figure 4E). Kyoto Encyclopedia of Genes and Genomes (KEGG) pathway analysis revealed apelin signaling pathway as the top enriched pathway. It was previously reported that *APLNR*, a fundamental gene in the apelin signaling pathway, is one of three genes that are sex biased through neural development in humans (Shi et al., 2016). Axon guidance, and pathways related to synaptic signaling, such as calcium signaling, dopaminergic, GABAergic and glutamatergic synapses were also enriched, in line with differences found in fetal human brains and during the early childhood period (O'Brien et al., 2019; Shi et al., 2016). In addition, during early neural development sex-biased genes were enriched for amyotrophic lateral sclerosis (ALS), autism spectrum disorder (ASD), and Rett syndrome gene sets, conditions known to have sex-bias phenotypes (Figure 4E). Taken together, these findings suggest that sex differences during human neural development are related to sex chromosome complement and are independent of hormonal differences that occur later in development.

DISCUSSION

Biological sex is one of the most fundamental and evolutionarily well-conserved phenomenon. Nevertheless, lack of a biological model in humans has impeded the study of sex biology. Development of a platform to study sex differences in humans will be valuable for understanding the impact of sex on development, disease pathogenesis and medical treatments. This study established an *in vitro* model for studying sex differences by generating human isogenic iPSC lines with different sex chromosome complements. Using this model, sex differences were studied in pluripotent stem cells and early-stage differentiated neural cells. Known and novel differences between the sexes were detected in the expression of both autosomal and sex chromosomes genes. In addition, female hiPSCs were shown to be more closely related to an earlier naive pluripotency state than their male counterparts. Taken together, the cellular model developed here enabled discovery of sex differences and their linkage to X versus Y chromosomes.

Genetic background can easily mask sex differences, subsequently requiring large sample sizes to establish such differences (Melé et al., 2015; Ronen and Benvenisty, 2014). The isogenic hiPSCs developed here eliminated the genetic background variability, and consequently enabled the detection of sex differences using only a few cell lines for each sex. The gene expression analysis in the pluripotent state and the main finding reported here regarding the difference in pluripotent states between the two sexes were validated using microarray data from multiple conventional hESC lines. In addition, the data demonstrating that estrogen response is sexually dimorphic and attributed to a Y chromosome effect aligned with the observations following a similar analysis of conventional hESCs (Ronen and Benvenisty, 2014).

Functional analysis of the DEGs revealed enrichment for biological functions such as estrogen response, glycolysis, and adipogenesis, all of which are known to be sexually dimorphic (Chen et al., 2012; Kimura et al., 2005; Ronen and Benvenisty, 2014). Immune response pathways were also differentially expressed, consistent with the suggested role of sex chromosome complement on immune system functions and the higher risk for autoimmune diseases in cases of sex chromosome aneuploidy (Harris et al., 2016; Jaillon et al., 2019; Sawalha et al., 2009; Schurz et al., 2019). Sex differences can arise from the presence of Y chromosome or X dose. Isogenic hiPSCs enabled differentiation between the effects of X and Y chromosomes on DEGs and biological processes. In line with previous reports (Chen et al., 2012; Ronen and Benvenisty, 2014), the present analysis attributed differences in the estrogen response pathway to the presence of Y, while adipogenesis was affected by X dose.

It was previously shown that female mouse ESCs cultured under serum/LIF conditions are more similar to the naive pluripotent state than their male counterparts due to two active Xs (Schulz et al., 2014; Zvetkova et al., 2005). In the human feeder-dependent culture conditions applied

here, female hiPSCs were X inactivated. Nevertheless, XX hiPSCs were enriched for the expression of naive markers, while primed pluripotency markers were enriched in XY hiPSCs. This effect was attributed to X dose as well as to Y presence. The enrichment of naive state markers in XX samples was validated using conventional hESC samples. The signaling pathways that differed between the sexes—JAK/STAT3, PI3K/AKT, and WNT—were upregulated in the naive state and might be responsible for the resemblance of XX hiPSCs to the naive pluripotency state. MAPK was also enriched in female hiPSCs, as opposed to its inhibition in the naive state, which might be due to the X inactivation of the cell lines (Schulz et al., 2014). These gene expression profiles suggest that although female and male hiPSCs are in the primed state, human female iPSCs are in an earlier pluripotency stage than their male counterparts. In line with these findings, it was previously reported that Y-linked genes downregulate naive state genes in human pluripotent stem cells (Taleahmad et al., 2019). In addition, regulation of the pluripotency network may be distinct for each sex, as demonstrated for SRY, which upregulates OCT4 in males, while ZFX, an X-linked gene that escapes X inactivation, has a role in self-renewal and pluripotency maintenance (Galan-Caridad et al., 2007).

The hiPSC model was effectively applied to analyze sex differences in differentiated cells. During early neuralization, most of the DEGs were upregulated in XY NPCs, as was shown in the prenatal human brain (Shi et al., 2016). Functional annotation analysis found enrichment for the synaptic compartment and specific neurotransmitters, differences that were also found during second trimester fetal development (O'Brien et al., 2019). Gene sets representing neurological diseases that are more prevalent in one sex, such as ALS, autism, and Rett syndrome, were found to be enriched within the sex-biased genes. Defects in oxidation-related genes are known to be related to ALS; for example, a mutation in the *SOD1* gene has been linked with familial ALS (Rosen et al., 1993). In addition, male rat NPCs harboring this mutation exhibit sex-specific effects on proliferation and sensitivity to oxidative stress (Li et al., 2012). In line with these findings, female and male NPCs in the present analysis exhibited differential expression of redox state response genes. Investigating the sex-biased effect of *SOD1* mutation in human NPCs using gene editing in our isogenic hiPSCs might contribute to the understanding of the sex-related pathogenesis of ALS. In conclusion, our system enables the detection of sex differences during development and within somatic cells. Moreover, it allowed the identification of sex differences during neural development earlier than previously reported. These differences can be attributed solely to sex chromosome complement, as no hormonal effects are involved during this early developmental stage.

The studied isogenic hiPSCs with different sex chromosome complements all harbored a single genetic background. Nevertheless, variability in gene expression existed because of subtle differences in culture conditions, batch effects, and possibly in the extent of X chromosome inactivation between the cell lines. In future studies, multiple technical replicates, and simultaneous RNA extraction from all cell lines might reduce this variability. Additional isogenic cell lines with different genetic backgrounds may be derived by reprogramming somatic cells of additional mosaic Klinefelter syndrome patients. Indeed, isogenic hiPSC lines with different sex chromosome complements (46,XY and 47,XXY) were previously derived from a mosaic Klinefelter syndrome patient. However, since these lines lacked a 46,XX hiPSC clone, they were not suitable to study sex differences (Fiacco et al., 2020). Sex chromosomes jettisoning during reprogramming of 47,XXY cells (Hirota et al., 2017) can facilitate the generation of additional isogenic hiPSC lines as well. Although the hiPSC system in the current work was based on a single genetic background, sex differences in undifferentiated and differentiated states that were previously reported using numerous samples, were recapitulated, which strengthened the validity of our system.

Although it is now broadly recognized that gender-specific medicine is needed, no suitable biological platform to pursue research in this direction exists. The unique isogenic hiPSC-based system with different sex chromosome complements developed here serves as the first human model for sex differences. This system may enable the study of sex differences in various medical conditions such as autism (Mitra et al., 2016), cardiovascular disease (Arnold et al., 2017) and autoimmune diseases (Whitacre, 2001). It will also serve as a platform for studying the role and molecular mechanism of sex-specific genetic variants and adverse drug effects (Pollitzer, 2013). In addition, it differentiates between the roles of X and Y chromosomes in sex differences and facilitate the understanding of hormonal versus chromosomal effects. Taken together, isogenic hiPSCs may serve as a novel means to study human sex differences, shedding light on the role of sex in health and disease, and will enrich gender medicine.

EXPERIMENTAL PROCEDURES

Additional methods and more detailed descriptions can be found in supplemental experimental procedures.

Resource availability

Corresponding author
Benjamin E. Reubinoff, benr@hadassah.org.il.

Materials availability

The isogenic iPSCs generated in this study will be made available for research upon completed Materials Transfer Agreement with Coriell Institute and the corresponding author's institution.

Data and code availability

RNA-seq datasets were deposited at Gene Expression Omnibus (GEO) with accession numbers GSE145079 and GSE145118.

Cell culture

EBV-immortalized B cells were obtained from Coriell cell repositories and cultured according to Coriell's recommended protocol. iPSCs were plated on growth factor-reduced Matrigel (Corning) in mTesr1 medium (STEMCELL Technologies) and expanded mechanically. Later, the cells were passaged to KO medium (Thermo Fisher Scientific) on human foreskin fibroblasts, as described previously (Ben-Dor et al., 2006).

Reprogramming EBV-immortalized B cells to iPSCs

B cells were reprogrammed as described by Barrett et al. (2014). Briefly, 1×10^6 B cells were nucleofected using B-Cell Nucleofector Kit (VPA-1001; Lonza) with 4 plasmids containing the following genes: SOX2, OCT4, KLF4, LIN28A, MYCL, SV40LT, and shTP53 (Addgene).

Neural differentiation

For differentiation, 10^4 cells per well were plated in non-treated 96-well plates with NPC differentiation medium composed of NutriStem(−) medium supplemented with HSA (20 μM/mL), bFGF (20 ng/mL), LDN (100 nM), and SB431542 (5 μM) (all from PeproTech). Rock inhibitor (10 μM; PeproTech) was added on day 0 only. Medium was changed on day 2 and then twice a week. After day 5, cells were cultured in differentiation medium without SB431542. NutriStem(−) was replaced by phenol red-free DMEM/F12 medium to eliminate hormonal effects at this time.

Copy number variation assay

TaqMan Copy Number Assays (Thermo Fisher Scientific) were used with probes for SRY on the Y chromosome and XIST and ARSH on the X chromosomes (Hs01026408_cn, Hs04111313_cn, and Hs00622494_cn, respectively). Each sample was subjected to duplex TaqMan qRT-PCR according to Applied Biosystems protocol. All reactions were run in triplicates. Data were analyzed using CopyCaller version 2.1 software (Applied Biosystems). XX and XY blood cells were used as control samples.

Short tandem repeat fingerprinting and human leukocyte antigen testing

STR profiles of 16 sites (D13S317, D7S820, D16S539, vWA, TH01, TPOX, CSF1PO, D8S1179, D21811, D19S433, D18851, D3S1358, D2S1338, D5S818, FGA, and amelogenin) were obtained using the IdentiFiler kit (Applied Biosystems). For HLA profiling, HLA-A, HLA-B, and DRB1 loci at low resolution were typed using Lifecodes HLA SSO Typing Kit (Immucor).

cDNA library preparation, deep sequencing, and bioinformatics analysis

One sample of total RNA was extracted from three hiPSC cell lines of 46,XX and 46,XY, two cell lines of 47,XXY and one 45,X0 line (passages 16–25). Total RNA was extracted from NPCs derived from three cell lines of 46,XX and 46,XY; each tested sample was a pooled sample of two differentiation experiments (passages 18–30). RNA was extracted using the miRNeasy Micro Kit (Qiagen). mRNA libraries were prepared from 1 mg RNA using the KAPA Stranded mRNA-Seq Kit, with mRNA Capture Beads (KK8421; Kapa Biosystems). The pooled multiplex samples were loaded on a NextSeq 500/550 High Output version 2 kit (75 cycles) cartridge and loaded on a NextSeq 500 System (Illumina). Normalization and differential expression were done with the DESeq2 package (Love et al., 2014) (version 1.6.3) of the Bioconductor project, separately for each sample. Testing was done with default parameters, using the Wald test with a significance threshold of adjusted $p < 0.10$. Correction for multiple comparisons was performed using the Benjamini-Hochberg procedure. Pathway and molecular function enrichment analysis of the significant DEGs (false discovery rate [FDR] < 0.1) was carried out using Qiagen's Ingenuity Pathway Analysis. Chromosome enrichment was tested using DAVID (Huang et al., 2009). Whole differential expression data were subjected to gene set enrichment analysis using GSEA (Subramanian et al., 2005). Gene sets from the hallmark collection of the molecular signatures database (MSigDB version 6.2; http://www.gsea-msigdb.org/gsea/msigdb/collections.jsp) as well as additional gene sets, related to pluripotency were used for GSEA. Threshold used were FDR < 0.01 and FWER < 0.1, with >80% of core enrichment genes in the correct direction. The isogenicity of hiPSC lines was tested using NGSCheckMate (Lee et al., 2017).

For NPC bioinformatic analysis, gene set over-representation analysis was performed with the WebGestaltR R-based package for gene set analysis (Liao et al., 2019), and with EnrichR web tool (Kuleshov et al., 2016). A set of DEGs was submitted after pre-filtering reduced fold change of at least 25% and $p \leq 0.01$.

SUPPLEMENTAL INFORMATION

Supplemental information can be found online at https://doi.org/10.1016/j.stemcr.2022.10.017.

AUTHOR CONTRIBUTIONS

Study Conception and Design, I.W. and B.E.R.; Experiment Conduct and Data Analysis, I.W., T.T., D.S., Y.G., and M.G.; Bioinformatic Analyses, H.B.; Manuscript Writing and Revision, I.W., B.E.R., and M.G.

ACKNOWLEDGMENTS

The study was supported by generous donations of Sidney and Judy Swartz, and Dan and Morrine Marantz, for the Stem Cells for Women's Health Initiative. RNA-seq was performed by the Genomic Applications Laboratory, The Core Research Facility, The Faculty of Medicine - Ein Kerem, The Hebrew University of Jerusalem, Israel. HLA and STR tests were performed by the Tissue Typing Laboratory, Hadassah Medical Organization. We would

like to thank Jonathan Monin, Prof. Michael Steinitz, and Prof. Howard Cedar for their contribution to this manuscript.

CONFLICTS OF INTEREST

B.E.R. is a member of the journal's Editorial Board. B.E.R. is a founder of, holds shares in, and is the chief scientific officer of CellCure Neuroscience Ltd. The company did not fund the study presented in this paper and has no interest in its results. A patent application related to the data presented in this paper has been submitted.

Received: November 15, 2021
Revised: October 26, 2022
Accepted: October 30, 2022
Published: November 24, 2022

REFERENCES

Al-Awadi, S.A., Teebi, A.S., Krishna Murthy, D.S., Othman, G., and Sundareshan, T.S. (1986). Klinefelter's syndrome, mosaic 46, XX/46, XY/47, XXY/48, XXXY/48, XXYY: a case report. Ann. Genet. *29*, 119–121.

Arnold, A.P. (2012). The end of gonad-centric sex determination in mammals. Trends Genet. *28*, 55–61.

Arnold, A.P., Cassis, L.A., Eghbali, M., Reue, K., and Sandberg, K. (2017). Sex hormones and sex chromosomes cause sex differences in the development of cardiovascular diseases. Arterioscler. Thromb. Vasc. Biol. *37*, 746–756.

Barrett, R., Ornelas, L., Yeager, N., Mandefro, B., Sahabian, A., Lenaeus, L., Targan, S.R., Svendsen, C.N., and Sareen, D. (2014). Reliable generation of induced pluripotent stem cells from human lymphoblastoid cell lines. Stem Cells Transl. Med. *3*, 1429–1434.

Ben-Dor, I., Itsykson, P., Goldenberg, D., Galun, E., and Reubinoff, B.E. (2006). Lentiviral vectors harboring a dual-gene system Allow high and homogeneous transgene expression in selected polyclonal human embryonic stem cells. Mol. Ther. *14*, 255–267.

Bergman, S., Nowakowski, H., and Reitalu, J. (1969). Cytological and clinical observations in XXY-XX-XY-XO mosaicism. Hereditas *61*, 276–278.

Bernardi, M.L., and Delouis, C. (1996). Sex-related differences in the developmental rate of in-vitro matured/in-vitro fertilized ovine embryos. Hum. Reprod. *11*, 621–626.

Case, L.K., Wall, E.H., Dragon, J.A., Saligrama, N., Krementsov, D.N., Moussawi, M., Zachary, J.F., Huber, S.A., Blankenhorn, E.P., and Teuscher, C. (2013). The y chromosome as a regulatory element shaping immune cell transcriptomes and susceptibility to autoimmune disease. Genome Res. *23*, 1474–1485.

Charchar, F.J., Bloomer, L.D., Barnes, T.A., Cowley, M.J., Nelson, C.P., Wang, Y., Denniff, M., Debiec, R., Christofidou, P., Nankervis, S., et al. (2012). Inheritance of coronary artery disease in men: an analysis of the role of the y chromosome. Lancet *379*, 915–922.

Chen, X., McClusky, R., Chen, J., Beaven, S.W., Tontonoz, P., Arnold, A.P., and Reue, K. (2012). The number of X chromosomes causes sex differences in adiposity in mice. PLoS Genet. *8*, e1002709.

Chounti, A., Hägglund, G., Wagner, P., and Westbom, L. (2013). Sex differences in cerebral palsy incidence and functional ability: a total population study. Acta Paediatr. *102*, 712–717.

Collier, A.J., Panula, S.P., Schell, J.P., Chovanec, P., Plaza Reyes, A., Petropoulos, S., Corcoran, A.E., Walker, R., Douagi, I., Lanner, F., and Rugg-Gunn, P.J. (2017). Comprehensive cell surface protein profiling identifies specific markers of human naive and primed pluripotent states. Cell Stem Cell *20*, 874–890.e7.

Costantine, M.M., Clark, E.A.S., Lai, Y., Rouse, D.J., Spong, C.Y., Mercer, B.M., Sorokin, Y., Thorp, J.M., Ramin, S.M., Malone, F.D., et al. (2012). Association of polymorphisms in neuroprotection and oxidative stress genes and neurodevelopmental outcomes after preterm birth. Obstet. Gynecol. *120*, 542–550.

Duggal, G., Warrier, S., Ghimire, S., Broekaert, D., Van Der Jeught, M., Lierman, S., Deroo, T., Peelman, L., Van Soom, A., Cornelissen, R., et al. (2015). Alternative routes to induce naïve pluripotency in human embryonic stem cells. Stem Cell. *33*, 2686–2698.

Ekwall, B., Bergman, S., and Reitalu, J. (1971). Karyotype XX/XY/XXY/XXXY in a klinefelter patient. Hereditas *69*, 140–145.

Fiacco, E., Alowaysi, M., Astro, V., and Adamo, A. (2020). Derivation of two naturally isogenic iPSC lines (KAUSTi006-A and KAUSTi006-B) from a mosaic Klinefelter Syndrome patient (47-XXY/46-XY). Stem Cell Res. *49*, 102049.

Frühmesser, A., and Kotzot, D. (2011). Chromosomal variants in klinefelter syndrome. Sex Dev. *5*, 109–123.

Gafni, O., Weinberger, L., Mansour, A.A., Manor, Y.S., Chomsky, E., Ben-Yosef, D., Kalma, Y., Viukov, S., Maza, I., Zviran, A., et al. (2013). Derivation of novel human ground state naive pluripotent stem cells. Nature *504*, 282–286.

Galan-Caridad, J.M., Harel, S., Arenzana, T.L., Hou, Z.E., Doetsch, F.K., Mirny, L.A., and Reizis, B. (2007). Zfx controls the self-renewal of embryonic and hematopoietic stem cells. Cell *129*, 345–357.

Ge, T., Chen, C.Y., Neale, B.M., Sabuncu, M.R., and Smoller, J.W. (2017). Phenome-wide heritability analysis of the UK Biobank. PLoS Genet. *13*, e1006711.

Giulitti, S., Pellegrini, M., Zorzan, I., Martini, P., Gagliano, O., Mutarelli, M., Ziller, M.J., Cacchiarelli, D., Romualdi, C., Elvassore, N., and Martello, G. (2019). Direct generation of human naive induced pluripotent stem cells from somatic cells in microfluidics. Nat. Cell Biol. *21*, 275–286.

Greenwood, T.A., Lazzeroni, L.C., Calkins, M.E., Freedman, R., Green, M.F., Gur, R.E., Gur, R.C., Light, G.A., Nuechterlein, K.H., Olincy, A., et al. (2016). Genetic assessment of additional endophenotypes from the consortium on the genetics of schizophrenia family study. Schizophr. Res. *170*, 30–40.

Guo, G., Von Meyenn, F., Santos, F., Chen, Y., Reik, W., Bertone, P., Smith, A., and Nichols, J. (2016). Naive pluripotent stem cells derived directly from isolated cells of the human inner cell mass. Stem Cell Rep. *6*, 437–446.

Gurvich, C., Hoy, K., Thomas, N., and Kulkarni, J. (2018). Sex differences and the influence of sex hormones on cognition through adulthood and the aging process. Brain Sci. *8*, 163.

Hao, Y., Liu, J., Liu, J., Yang, N., Smith, S.C., Jr., Huo, Y., Fonarow, G.C., Ge, J., Taubert, K.A., Morgan, L., et al. (2019). Sex differences in in-hospital management and outcomes of patients with acute

coronary syndrome: findings from the improving care for cardiovascular disease in China (CCC) project. Circulation *139*, 1776–1785.

Harris, V.M., Sharma, R., Cavett, J., Kurien, B.T., Liu, K., Koelsch, K.A., Rasmussen, A., Radfar, L., Lewis, D., Stone, D.U., et al. (2016). Klinefelter's syndrome (47, XXY) is in excess among men with Sjögren's syndrome. Clin. Immunol. *168*, 25–29.

Heid, I.M., Jackson, A.U., Randall, J.C., Winkler, T.W., Qi, L., Steinthorsdottir, V., Thorleifsson, G., Zillikens, M.C., Speliotes, E.K., Mägi, R., et al. (2010). Meta-analysis identifies 13 new loci associated with waist-hip ratio and reveals sexual dimorphism in the genetic basis of fat distribution. Nat. Genet. *42*, 949–960.

Hersmus, R., Stoop, H., Turbitt, E., Oosterhuis, J.W., Drop, S.L., Sinclair, A.H., White, S.J., and Looijenga, L.H. (2012). SRY mutation analysis by next generation (deep) sequencing in a cohort of chromosomal Disorders of Sex Development (DSD) patients with a mosaic karyotype. BMC Med. Genet. *13*, 108.

Hirota, T., Ohta, H., Powell, B.E., Mahadevaiah, S.K., Ojarikre, O.A., Saitou, M., and Turner, J.M.A. (2017). Fertile offspring from sterile sex chromosome trisomic mice. Science (80-.) *357*, 932–935.

Huang, D.W., Sherman, B.T., and Lempicki, R.A. (2009). Systematic and integrative analysis of large gene lists using DAVID bioinformatics resources. Nat. Protoc. *4*, 44–57.

Inanloorahatloo, K., Liang, G., Vo, D., Ebert, A., Nguyen, I., and Nguyen, P.K. (2017). Sex-based differences in myocardial gene expression in recently deceased organ donors with no prior cardiovascular disease. PLoS One *12*, e0183874.

Ingason, A., Giegling, I., Hartmann, A.M., Genius, J., Konte, B., Friedl, M., Schizophrenia Working Group of the Psychiatric Genomics Consortium PGC, Ripke, S., Sullivan, P.F., St Clair, D., et al. (2015). Expression analysis in a rat psychosis model identifies novel candidate genes validated in a large case-control sample of schizophrenia. Transl. Psychiatry *5*, e656.

Jaillon, S., Berthenet, K., and Garlanda, C. (2019). Sexual dimorphism in innate immunity. Clin. Rev. Allergy Immunol. *56*, 308–321.

Kamitaki, N., Sekar, A., Handsaker, R.E., de Rivera, H., Tooley, K., Morris, D.L., Taylor, K.E., Whelan, C.W., Tombleson, P., Loohuis, L.M.O., et al. (2020). Complement genes contribute sex-biased vulnerability in diverse disorders. Nature *582*, 577–581.

Khramtsova, E.A., Davis, L.K., and Stranger, B.E. (2019). The role of sex in the genomics of human complex traits. Nat. Rev. Genet. *20*, 173–190.

Kilens, S., Meistermann, D., Moreno, D., Chariau, C., Gaignerie, A., Reignier, A., Lelièvre, Y., Casanova, M., Vallot, C., Nedellec, S., et al. (2018). Parallel derivation of isogenic human primed and naive induced pluripotent stem cells. Nat. Commun. *9*, 360.

Kimura, K., Spate, L.D., Green, M.P., and Roberts, R.M. (2005). Effects of D-glucose concentration, D-fructose, and inhibitors of enzymes of the pentose phosphate pathway on the development and sex ratio of bovine blastocysts. Mol. Reprod. Dev. *72*, 201–207.

Krementsov, D.N., Case, L.K., Dienz, O., Raza, A., Fang, Q., Ather, J.L., Poynter, M.E., Boyson, J.E., Bunn, J.Y., and Teuscher, C. (2017). Genetic variation in chromosome y regulates susceptibility to influenza A virus infection. Proc. Natl. Acad. Sci. USA *114*, 3491–3496.

Kukurba, K.R., Parsana, P., Balliu, B., Smith, K.S., Zappala, Z., Knowles, D.A., Favé, M.J., Davis, J.R., Li, X., Zhu, X., et al. (2016). Impact of the X chromosome and sex on regulatory variation. Genome Res. *26*, 768–777.

Kuleshov, M.V., Jones, M.R., Rouillard, A.D., Fernandez, N.F., Duan, Q., Wang, Z., Koplev, S., Jenkins, S.L., Jagodnik, K.M., Lachmann, A., et al. (2016). Enrichr: a comprehensive gene set enrichment analysis web server 2016 update. Nucleic Acids Res. *44*, W90–W97.

Lee, S., Lee, S., Ouellette, S., Park, W.Y., Lee, E.A., and Park, P.J. (2017). NGSCheckMate: software for validating sample identity in Next-generation sequencing studies within and across data types. Nucleic Acids Res. *45*, e103.

Li, R., Strykowski, R., Meyer, M., Mulcrone, P., Krakora, D., and Suzuki, M. (2012). Male-specific differences in proliferation, neurogenesis, and sensitivity to oxidative stress in neural progenitor cells derived from a rat model of ALS. PLoS One *7*, e48581.

Liao, Y., Wang, J., Jaehnig, E.J., Shi, Z., and Zhang, B. (2019). WebGestalt 2019: gene set analysis toolkit with revamped UIs and APIs. Nucleic Acids Res. *47*, W199–W205.

Lichtman, J.H., Leifheit, E.C., Safdar, B., Bao, H., Krumholz, H.M., Lorenze, N.P., Daneshvar, M., Spertus, J.A., and D'Onofrio, G. (2018). Sex differences in the presentation and perception of symptoms among young patients with myocardial infarction. Circulation *137*, 781–790.

Love, M.I., Huber, W., and Anders, S. (2014). Moderated estimation of fold change and dispersion for RNA-seq data with DESeq2. Genome Biol. *15*, 550.

Mark, H.F., Bai, H., Sotomayor, E., Mark, S., Zolnierz, K., Airall, E., and Sigman, M. (1999). A variant klinefelter syndrome patient with an XXY/XX/XY karyotype studied by GTG-banding and fluorescence in situ hybridization. Exp. Mol. Pathol. *67*, 50–56.

McGrath, J., Saha, S., Welham, J., El Saadi, O., MacCauley, C., and Chant, D. (2004). A systematic review of the incidence of schizophrenia: the distribution of rates and the influence of sex, urbanicity, migrant status and methodology. BMC Med. *2*, 13.

Melé, M., Ferreira, P.G., Reverter, F., DeLuca, D.S., Monlong, J., Sammeth, M., Young, T.R., Goldmann, J.M., Pervouchine, D.D., Sullivan, T.J., et al. (2015). The human transcriptome across tissues and individuals-Supplementary Materials. Science (80-.) *348*, 660–665.

Messmer, T., von Meyenn, F., Savino, A., Santos, F., Mohammed, H., Lun, A.T.L., Marioni, J.C., and Reik, W. (2019). Transcriptional heterogeneity in naive and primed human pluripotent stem cells at single-cell resolution. Cell Rep. *26*, 815–824.e4.

Mitra, I., Tsang, K., Ladd-Acosta, C., Croen, L.A., Aldinger, K.A., Hendren, R.L., Traglia, M., Lavillaureix, A., Zaitlen, N., Oldham, M.C., et al. (2016). Pleiotropic mechanisms indicated for sex differences in autism. PLoS Genet. *12*, e1006425.

Nakamura, T., Okamoto, I., Sasaki, K., Yabuta, Y., Iwatani, C., Tsuchiya, H., Seita, Y., Nakamura, S., Yamamoto, T., and Saitou, M. (2016). A developmental coordinate of pluripotency among mice, monkeys and humans. Nature *537*, 57–62.

O'Brien, H.E., Hannon, E., Jeffries, A.R., Davies, W., Hill, M.J., Anney, R.J., O'Donovan, M.C., Mill, J., and Bray, N.J. (2019). Sex differences in gene expression in the human fetal brain. Preprint at bioRxiv. https://doi.org/10.1101/483636.

Pastor, W.A., Liu, W., Chen, D., Ho, J., Kim, R., Hunt, T.J., Lukianchikov, A., Liu, X., Polo, J.M., Jacobsen, S.E., and Clark, A.T. (2018). TFAP2C regulates transcription in human naive pluripotency by opening enhancers. Nat. Cell Biol. *20*, 553–564.

Pergament, E., Fiddler, M., Cho, N., Johnson, D., and Holmgren, W.J. (1994). Sexual differentiation and preimplantation cell growth. Hum. Reprod. *9*, 1730–1732.

Petropoulos, S., Edsgärd, D., Reinius, B., Deng, Q., Panula, S.P., Codeluppi, S., Plaza Reyes, A., Linnarsson, S., Sandberg, R., and Lanner, F. (2016). Single-cell RNA-seq reveals lineage and X chromosome dynamics in human preimplantation embryos. Cell *165*, 1012–1026.

Pollitzer, E. (2013). Biology: cell sex matters. Nature *500*, 23–24.

Ronen, D., and Benvenisty, N. (2014). Sex-dependent gene expression in human pluripotent stem cells. Cell Rep. *8*, 923–932.

Rosen, D.R., Siddique, T., Patterson, D., Figlewicz, D.A., Sapp, P., Hentati, A., Donaldson, D., Goto, J., O'Regan, J.P., Deng, H.X., et al. (1993). Mutations in Cu/Zn superoxide dismutase gene are associated with familial amyotrophic lateral sclerosis. Nature *362*, 59–62.

Sawalha, A.H., Harley, J.B., and Scofield, R.H. (2009). Autoimmunity and Klinefelter's syndrome: when men have two X chromosomes. J. Autoimmun. *33*, 31–34.

Schulz, E.G., Meisig, J., Nakamura, T., Okamoto, I., Sieber, A., Picard, C., Borensztein, M., Saitou, M., Blüthgen, N., and Heard, E. (2014). The two active X chromosomes in female ESCs block exit from the pluripotent state by modulating the ESC signaling network. Cell Stem Cell *14*, 203–216.

Schurz, H., Salie, M., Tromp, G., Hoal, E.G., Kinnear, C.J., and Möller, M. (2019). The X chromosome and sex-specific effects in infectious disease susceptibility. Hum. Genomics *13*, 2.

Shi, L., Zhang, Z., and Su, B. (2016). Sex biased gene expression profiling of human brains at major developmental stages. Sci. Rep. *6*, 21181.

Sperber, H., Mathieu, J., Wang, Y., Ferreccio, A., Hesson, J., Xu, Z., Fischer, K.A., Devi, A., Detraux, D., Gu, H., et al. (2015). The metabolome regulates the epigenetic landscape during naive-to-primed human embryonic stem cell transition. Nat. Cell Biol. *17*, 1523–1535.

Stirparo, G.G., Boroviak, T., Guo, G., Nichols, J., Smith, A., and Bertone, P. (2018). Integrated analysis of single-cell embryo data yields a unified transcriptome signature for the human pre-implantation epiblast. Development *145*, dev158501.

Subramanian, A., Tamayo, P., Mootha, V.K., Mukherjee, S., Ebert, B.L., Gillette, M.A., Paulovich, A., Pomeroy, S.L., Golub, T.R., Lander, E.S., and Mesirov, J.P. (2005). Gene set enrichment analysis: a knowledge-based approach for interpreting genome-wide expression profiles. Proc. Natl. Acad. Sci. USA *102*, 15545–15550.

Takata, A., Iwayama, Y., Fukuo, Y., Ikeda, M., Okochi, T., Maekawa, M., Toyota, T., Yamada, K., Hattori, E., Ohnishi, T., et al. (2013). A population-specific uncommon variant in GRIN3A associated with schizophrenia. Biol. Psychiatry *73*, 532–539.

Taleahmad, S., Alikhani, M., Mollamohammadi, S., Yousefi, M., Taei, A., Hassani, S.N., Baharvand, H., and Salekdeh, G.H. (2019). Inhibition of human Y chromosome gene, SRY, promotes naïve state of human pluripotent stem cells. J. Proteome Res. *18*, 4254–4261.

Theunissen, T.W., Powell, B.E., Wang, H., Mitalipova, M., Faddah, D.A., Reddy, J., Fan, Z.P., Maetzel, D., Ganz, K., Shi, L., et al. (2014). Systematic identification of culture conditions for induction and maintenance of naive human pluripotency. Cell Stem Cell *15*, 524–526.

Traglia, M., Bseiso, D., Gusev, A., Adviento, B., Park, D.S., Mefford, J.A., Zaitlen, N., and Weiss, L.A. (2017). Genetic mechanisms leading to sex differences across common diseases and anthropometric traits. Genetics *205*, 979–992.

Turano, A., Osborne, B.F., and Schwarz, J.M. (2018). Sexual differentiation and sex differences in neural development. Curr. Top. Behav. Neurosci. *43*, 69–110.

Valdivia, R.P., Kunieda, T., Azuma, S., and Toyoda, Y. (1993). PCR sexing and developmental rate differences in preimplantation mouse embryos fertilized and cultured in vitro. Mol. Reprod. Dev. *35*, 121–126.

Whitacre, C.C. (2001). Sex differences in autoimmune disease. Nat. Immunol. *2*, 777–780.

Winkler, T.W., Justice, A.E., Graff, M., Barata, L., Feitosa, M.F., Chu, S., Czajkowski, J., Esko, T., Fall, T., Kilpeläinen, T.O., et al. (2015). The influence of age and sex on genetic associations with adult body size and shape: a large-scale genome-wide interaction study. PLoS Genet. *11*, 10053788–e1005442.

Xu, Z., Robitaille, A.M., Berndt, J.D., Davidson, K.C., Fischer, K.A., Mathieu, J., Potter, J.C., Ruohola-Baker, H., and Moon, R.T. (2016). Wnt/β-catenin signaling promotes self-renewal and inhibits the primed state transition in naïve human embryonic stem cells. Proc. Natl. Acad. Sci. USA *113*, E6382–E6390.

Yang, J., Van Oosten, A.L., Theunissen, T.W., Guo, G., Silva, J.C.R., and Smith, A. (2010). Stat3 activation is limiting for reprogramming to ground state pluripotency. Cell Stem Cell *7*, 319–328.

Yu, Y., Chen, J., Li, D., Wang, L., Wang, W., and Liu, H. (2016). Systematic analysis of adverse event reports for sex differences in adverse drug events. Sci. Rep. *6*, 24955.

Zamora, L., Espinet, B., Salido, M., Solé, F., Ligorria, C., and Florensa, L. (2002). Report of 46, XX/46, XY/47, XXY/48, XXYY mosaicism in an adult phenotypic male. Am. J. Med. Genet. *111*, 215–217.

Zimmerlin, L., Park, T.S., Huo, J.S., Verma, K., Pather, S.R., Talbot, C.C., Agarwal, J., Steppan, D., Zhang, Y.W., Considine, M., et al. (2016). Tankyrase inhibition promotes a stable human naïve pluripotent state with improved functionality. Development *143*, 4368–4380.

Zvetkova, I., Apedaile, A., Ramsahoye, B., Mermoud, J.E., Crompton, L.A., John, R., Feil, R., and Brockdorff, N. (2005). Global hypomethylation of the genome in XX embryonic stem cells. Nat. Genet. *37*, 1274–1279.